Published in final edited form as:
*Angew Chem Int Ed Engl*. 2011 June 20; 50(26): 5839–5842. doi:10.1002/anie.201101225.

# Connecting chemotypes and phenotypes of cultured marine microbial assemblages using imaging mass spectrometry

**Yu-Liang Yang, Dr.**[+],
Skaggs School of Pharmacy and Pharmaceutical Sciences, University of California, San Diego, California, USA

**Yuquan Xu, Dr.**[+],
Skaggs School of Pharmacy and Pharmaceutical Sciences, University of California, San Diego, California, USA

**Roland Kersten**,
Center for Marine Biotechnology and Biomedicine, Scripps Institution of Oceanography, University of California, San Diego, California, USA

**Wei-Ting Liu**,
Department of Chemistry and Biochemistry, University of California, San Diego, California, USA

**Michael J. Meehan**,
Skaggs School of Pharmacy and Pharmaceutical Sciences, University of California, San Diego, California, USA

**Bradley S. Moore, Prof., Dr.**,
Skaggs School of Pharmacy and Pharmaceutical Sciences, University of California, San Diego, California, USA; Center for Marine Biotechnology and Biomedicine, Scripps Institution of Oceanography, University of California, San Diego, California, USA

**Nuno Bandeira, Prof. Dr.**, and
Skaggs School of Pharmacy and Pharmaceutical Sciences, University of California, San Diego, California, USA; Department of Computer Science and Engineering, University of California, San Diego, Calfornia, USA

**Pieter C. Dorrestein, Prof., Dr.**
Skaggs School of Pharmacy and Pharmaceutical Sciences, University of California, San Diego, California, USA; Center for Marine Biotechnology and Biomedicine, Scripps Institution of Oceanography, University of California, San Diego, California, USA; Department of Chemistry and Biochemistry, University of California, San Diego, California, USA, Biomedical Science Building (BSB), Room 4090, 9500 Gilman Drive, MC 0636, La Jolla, CA 92093-0636

Pieter C. Dorrestein: pdorrest@ucsd.edu

From the early days of bacterial culturing over a century ago, microbiologists have known that microorganisms respond to their surroundings. Unicellular organisms rely on metabolic exchange to adapt to environmental stresses, sense colony density, occupy niches within hosts and form biofilms.[1-7] For example, *Bacillus subtilis* utilizes metabolic exchange to lyse neighboring microbes, including siblings, during sporulation.[8-10] While other forms of metabolic exchange, such as siderophores, stimulate the growth and development of

Correspondence to: Pieter C. Dorrestein, pdorrest@ucsd.edu.

[+]These authors contributed equally.

Supporting information for this article is available on the www under http://www.angewandte.org or from the author.

*Streptomyces* and uncultured bacteria.[11, 12] Despite the importance of chemistry in biology, studies that connect chemotypes and phenotypes to adaptive microbial behavior in Petri-dishes, including signaling and chemical warfare, have largely been disconnected and measured indirectly. To connect the chemotypes and phenotypes in this study, MALDI-based imaging mass spectrometry (IMS)[13-16] was utilized to observe the chemical output and metabolic exchange of a marine microbial assemblage in two-dimensions. The capability to monitor the 2-dimensional distribution of a wide array of metabolites simultaneously from a complex mixture of distinct organisms opens the door to comprehensive analyses of interspecies signaling interactions within a microbial assemblage in a spatial fashion. Analyzing the spatial distribution of these metabolites enables one to generate a testable hypothesis, without the immediate need to know the structural characteristics, with respect to functions of the observed chemotypes. IMS provides the ability to correlate the presence of metabolites to phenotypic changes and to detect new chemotypes and/or phenotypes that cannot be observed by the naked eye. As such, IMS allows one to prioritize the molecules to be targeted for identification through proteomic and metabolomic approaches, or to be subjected to mass spectrometry guided isolation and nuclear magnetic resonance based structure elucidation. Understanding these molecular networks and interactions will illuminate how microbes respond to neighboring organisms and in turn influence and alter growth of their neighbors.

We demonstrate that IMS can be used to observe the chemical output within complex microbial assemblages. This information can then be used to prioritize the organisms and molecules for structural characterization. It is important to prioritize the molecules because the structural characterization of the molecules is one of the rate limiting steps in our understanding of chemical cross-talk between organisms. We collected the marine microbial assemblage by scraping the slimy surface of a barnacle located on the pier of the Scripps Institution of Oceanography (University of California, San Diego), which extends into the Pacific Ocean. IMS was used to visualize the interactions between members of the microbial assemblage obtained from this barnacle and grown on solid media. Because a typical soil sample contains $10^8$ colony forming units (CFUs) per-gram of soil, and an ocean sample typically contains $10^5$ CFUs/mL of water, we anticipated that we would observe large numbers of colonies from this environmental sample. Therefore the barnacle scrapings were serially diluted onto agar plates. Subsequently the heterogeneous mixture of microorganisms was allowed to grow at 28 °C for 3 days (Figure 1a). Once distinct colonies were visible, a region of 4 cm by 2 cm of agar was cut, laid on top of a MALDI target plate and covered with a matrix of α-cyano-4-hydroxy-cinnamic acid and 2,5-dihydroxybenzoic acid. The matrix is required for the ionization of the molecules present along the surface of the sample. At the same time, the matrix effectively fixes the organisms in place when applied. Once covered with a coating of matrix, the sample was subjected to IMS. IMS enables the visualization of both metabolites that are secreted into the growth media, as well as metabolites associated with the colonies themselves. Nine signals and their distributions are highlighted in Figure 1c. In this figure each ion distribution is superimposed over the selection of Figure 1a enclosed in the rectangle. Five of the signals are associated with colonies and four of them are secreted into the agar medium. Based on the imaging data alone, two organisms from the marine sample that influenced each other's physiology were investigated more closely.

The IMS data suggested that one secreted metabolite with a mass of 2869 Da from organism SIO-11 (Scripps Institution of Oceanography-organism 11) inhibited the motility of organism SIO-1. The interactions observed between these two organisms were confirmed when they were grown in isolation from the rest of the microbial assemblage: SIO-11 inhibited the motility of a monoculture SIO-1 via the secretion of a metabolite (*m/z* 2869) and at the same time, the presence of SIO-1 resulted in the production of additional

metabolites (*m/z* 727, 729, 743, 765, 781, and 796) in SIO-11 in a time dependent manner originating at the juncture where the two organisms physically interact (Figure 2a). When SIO-11 was grown by itself for 120 hours, only the molecules with a mass of 2869 Da was observed (Supplementary Figure 20). This example illustrates the multifaceted nature of microorganism interactions and that IMS provides testable hypotheses. As such, IMS allowed prioritization of both 2869 and 743 for further structural and functional characterization.

We then sought to identify the signals observed by IMS (Figure 1). Here the species information based on 16S rDNA sequencing was directly informative, as our lab had previously characterized the metabolic output of *B. subtilis*, which was identical in 16S rDNA to SIO-1 (Supplementary Figure 5)[15]. Indeed, the mass spectral profile of SIO-1 was remarkably similar to *B. subtilis* 3610, and the ions at *m/z* 714 (partially characterized polyglutamate), 1075 (surfactin), 1545 (Plipastatin), *m/z* 3475 (subtilosin) as confirmed by via TOF/TOF analysis, can be observed in both strains. (Supplementary Figures 6-8).[15] In addition, there are several metabolites that were associated with other colonies. Tandem MS analysis identified one metabolite (*m/z* 843) to be related to the polyglutamate (*m/z* 714) but with an additional glutamate (Supplementary Figure 9). Based on their distribution, these polyglutamates may be components of extracellular matrix or cell wall material. Among the most interesting signals by IMS, however, were the unknown molecules secreted by SIO-11 (with an *m/z* at 2869) because it overlaps with the region where SIO-1 did not grow, and six additional molecular mass spectrometry signals at *m/z* 727, 729, 743, 765, 781, and 796 which are observed when SIO-11 is cultured adjacent to SIO-1.

In order to obtain the unknown metabolites for further structural and functional characterization, 72 h cultures of SIO-11 grown in A1 media at 28 °C were extracted with MeOH and acetone, then purified via mass spectrometry-guided isolation involving size-exclusion and reversed-phase chromatography. Purified peptide 2869 inhibited the motility of *B. subtilis* SIO-1 with as little as 0.035 nmol spotted onto an agar plate (Figure 2b). High resolution mass spectrometry (FT-ICR-MS) data indicated that the observed neutral monoisotopic mass was 2866.65 Da (Supplementary Figure 10). Because the genome for SIO-11 is not available, peptide 2869 was subjected to multiple stages of tandem mass spectrometry and, in combination with Spectral Networks (Supplementary Figure 12), a proteomics algorithm that enables the alignment and *de novo* sequencing of multistage tandem mass spectrometry data[17, 18], and it was determined to be a peptide. The sequence was determined by *de novo* sequencing and NMR interpretation as MSVVDIVSTLLDSLGITIAQLRVLIGL with an N-formyl group at methionine (Supplementary Figures 11-19, and Supplementary Tables 1-2). Because the peptide 2869 did not suppress growth of SIO-1, the data implies that the function of this peptide, produced by the non-motile SIO-11, is to prevent mobile bacteria, such as a motile *B. subtilis*, from entering its growth niche (Supplementary Figure 4). From an ecological standpoint, the inhibition of motility represents a creative approach for a non-motile bacterium to protect itself and to establish a colony among other motile bacteria (Figure 2b and c).

Because several metabolites produced by SIO-11 were only up-regulated in the presence of SIO-1, they were quite difficult to isolate in high enough quantity for structural elucidation. Therefore, 600 100 mm agar plates containing co-cultured SIO-1 and SIO-11 were prepared. Subsequently, the cells at the interface of the two organisms were harvested and extracted. Following gel filtration and HPLC purification, compounds with a mass of 743 Da as well as 796 Da (Figure 2d) were isolated. The mass difference from the IMS observed signals at *m/z* 743, 765, and 781 were due to a sodium ion and a potassium ion that were removed during purification. It was not immediately clear why there was an observed mass at *m/z* 796 until the sample was analyzed by high resolution mass spectrometry. High resolution

mass spectrometry (FT-ICR-MS) provided two major masses, one at *m/z* 743.5678 $[M+H]^+$ and another signal at *m/z* 796.4774. These masses provided the molecular formulas $C_{38}H_{74}N_6O_8$, $C_{38}H_{71}N_6O_8Fe$ and provided the first indication that this ion was an iron chelator, also known as siderophore[8]. In addition the 796.4774 displayed the characteristic iron isotopic profile (Supplementary Figure 27). We named this compound promicroferrioxamine because of the functional and structural similarity to the commercially utilized desferrioxamine and the 16S rDNA phylogenetic analysis of the producing organism (Supplementary Figure 5)[11]. Microorganisms of marine origin often produce siderophores that are key components for establishing microbial communities[12, 19]. The compounds with masses of *m/z* 727 and 729 are structurally related to promicroferrioxamine, thus SIO-11 secreted an array of siderophores in response to the presence of SIO-1 (Supplementary Figures 29-32).

To determine the structure of promicroferrioxamine, an estimated 7.3 μg of purified material was subjected to nanomole-scale NMR analysis (Supplementary Figure 3)[20]. The TOCSY, COSY, and HMBC spectra revealed three sets of cadaverines and two sets of succinyl moieties (Supplementary Figures 22-26). The long-range proton carbon correlations between the methylene of cadaverine and the carbonyl group of succinyl moiety indicate cadaverine and succinyl moieties are connected by an amide bond. Taking the fragment formula deduced from $FTMS^2$ into consideration, the hydroxyl group was assigned to be the substitute of nitrogen in cadaverine, resulting in the hydroxamate group (Supplementary Figure 28). The remaining NMR signals were elucidated as an *anteiso* containing alkyl chain and the chain length was confirmed via fragmentation and molecular formula (Supplementary Table 3). Thus, the structure of promicroferrioxamine is determined as a hydroxamate siderophore (Figure 2e). Based on the structure, the calculated mass (743.5646 Da, $[M+H]^+$) was within 0.0032 Da as observed by high-resolution mass spectrometry.

The IMS of this marine environmental sample enabled direct observation of numerous molecular signals. Two such molecules involved in metabolic exchange, previously uncharacterized, were further investigated and found to have different functions. First, we identified a peptide that prevents neighboring organisms from migrating into its producer's territory, a functional phenotype not observed in liquid cultures, while the second, a metabolite, is produced when there is competition for resources such as iron. The data suggest that such iron competition may also exist in growth conditions with sufficient iron. In this study, we observed that promicroferrioxamine, a hydroxamate siderophore, is produced by *Promicromonosporaceae* strain SIO-11 in response to the presence of *B. subtilis* SIO-1. This competition also exists in liquid media where we see the production of promicroferrioxamine in response to the addition of SIO-1 (Supplementary Figure 21). These are two examples of molecules involved in metabolic exchange found on the back of a barnacle, and underscore the many different chemical entities that exist within environmental microbial interactions. Here we show that IMS enables the visualization of such interactions in a microbial assemblage and that these signals are independent of their function and structural classification.

## Supplementary Material

Refer to Web version on PubMed Central for supplementary material.

## Acknowledgments

**

The funding of Dorrestein Lab was provided by the Beckman Foundation, NIH grants GM085770 (B.S.M) 1-P41-RR024851 (NB) and NIH GM08283 (P.C.D.). W.-T.L. was supported, in part, by a study aboard grant

SAS-98116-2-US-108 from Taiwan. Authors would like to thank Elizabeth Shank for critically reviewing the manuscript.

## References

1. Bassler BL, Losick R. Cell. 2006; 125:237–246. [PubMed: 16630813]
2. Straight PD, Kolter R. Annu Rev Microbiol. 2009; 63:99–118. [PubMed: 19566421]
3. Dudler R, Eberl L. Curr Opin Biotechnol. 2006; 17:268–273. [PubMed: 16650977]
4. Scherlach K, Hertweck C. Org Biomol Chem. 2009; 7:1753–1760. [PubMed: 19590766]
5. Shank EA, Kolter R. Curr Opin Microbiol. 2009; 12:205–214. [PubMed: 19251475]
6. Pacheco AR, Sperandio V. Curr Opin Microbiol. 2009; 12:192–198. [PubMed: 19318290]
7. Schroeckh V, Scherlach K, Nützmann HW, Shelest E, Schmidt-Heck W, Schuemann J, Martin K, Hertweck C, Brakhage AA. Proc Natl Acad Sci U S A. 2009; 106:14558–14563. [PubMed: 19666480]
8. Liu WT, Yang YL, Xu Y, Lamsa A, Haste NM, Yang JY, Ng J, Gonzalez D, Ellermeier CD, Straight PD, Pevzner PA, Pogliano J, Nizet V, Pogliano K, Dorrestein PC. Proc Natl Acad Sci U S A. 2010; 107:16286–16290. [PubMed: 20805502]
9. Ellermeier CD, Hobbs EC, Gonzalez-Pastor JE, Losick R. Cell. 2006; 124:549–559. [PubMed: 16469701]
10. González-Pastor JE, Hobbs EC, Losick R. Science. 2003; 301:510–513. [PubMed: 12817086]
11. Yamanaka K, Oikawa H, Ogawa HO, Hosono K, Shinmachi F, Takano H, Sakuda S, Beppu T, Ueda K. Microbiology. 2005; 151:2899–2905. [PubMed: 16151202]
12. D'Onofrio A, Crawford JM, Stewart EJ, Witt K, Gavrish E, Epstein S, Clardy J, Lewis K. Chem Biol. 2010; 17:254–264. [PubMed: 20338517]
13. Cornett DS, Reyzer ML, Chaurand P, Caprioli RM. Nat Methods. 2007; 4:828–833. [PubMed: 17901873]
14. Chughtai K, Heeren RM. Chem Rev. 2010; 110:3237–3277. [PubMed: 20423155]
15. Yang YL, Xu Y, Straight P, Dorrestein PC. Nat Chem Biol. 2009; 5:885–887. [PubMed: 19915536]
16. Svatos A. Trends Biotechnol. 2010; 28:425–434. [PubMed: 20580110]
17. Bandeira N, Clauser KR, Pevzner PA. Mol Cell Proteomics. 2007; 6:1123–34. [PubMed: 17446555]
18. Bandeira N, Olsen JV, Mann JV, Mann M, Pevzner PA. Bioinformatics. 2008; 24:416–23.
19. Vraspir JM, Butler A. Annu Rev Mar Sci. 2009; 1:43–63.
20. Dalisay DS, Molinski TF. J Nat Prod. 2009; 72:739–744. [PubMed: 19399996]

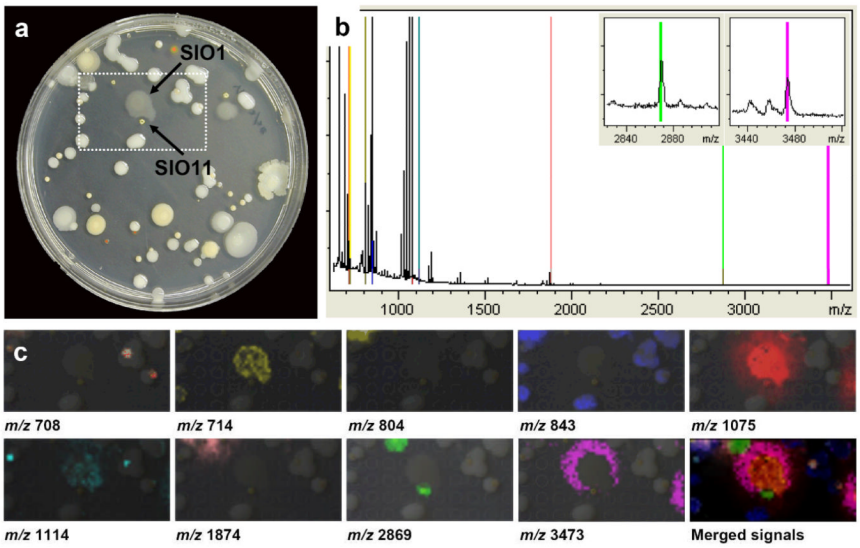


**Figure 1. The source and the visualization of the chemical output of the marine microbial assemblage**

(a) A photograph of the microorganisms isolated from the slimy layer of the barnacles, which were grown on ISP-2 containing Petri-dish (100 mm × 15 mm). (b) Average mass spectrum of a total of 1681 spectra collected during the IMS experiment. The observed ions that were visualized using different colors are highlighted. (c) Spatial distribution of the signals. The mass corresponding to the ions is provided below the images. In these images the most abundant ions are shown with a 1 Da window.

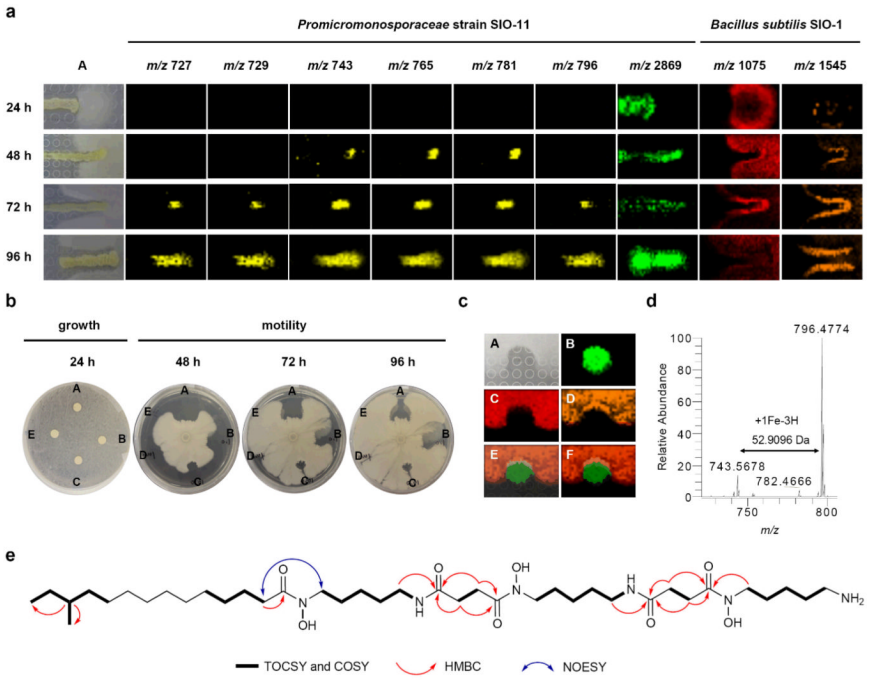


**Figure 2. The interaction between *Bacillus subtilis* SIO-1 and *Promicromonosporaceae* strain SIO-11**

(a) Time course IMS of SIO-1 and SIO-11 co-cultures. The siderophores (*m/z* 727 $[M+H]^+$, 729 $[M+H]^+$, 743 $[M+H]^+$, 765 $[M+Na]^+$, 781 $[M+K]^+$, 796 $[M+Fe-2H]^+$) and the peptide 2869 (*m/z* 2869 $[M+H]^+$) were produced by SIO-11. Surfactin (*m/z* 1075 $[M+K]^+$) and plipastatin (*m/z* 1545 $[M+K]^+$) were produced by SIO-1. Promicroferrioxamine (*m/z* 743 $[M+H]^+$, 765 $[M+Na]^+$, and 781 $[M+K]^+$) was observed after 48-hour co-culturing and the iron-chelating signal *m/z* 796 $[M+Fe-2H]^+$ was observed after 72-hours. Two additional siderophores (*m/z* 727 $[M+H]^+$ and 729 $[M+H]^+$) were detected after 72-hour co-culturing. These ions are not observed in SIO-11 when cultured alone on the agar based media (Supplementary Figure 20). In these images, the IMS signals are shown with a 1 Da window. A is a photograph of the colonies. (b) Functional evaluation of the peptide 2869 from SIO-11. The growth of SIO-1 was not affected by the peptide 2869 at 24 h. The motility of SIO-1 was halted when SIO-1 reached the spot treated with 10 μg, 1μg and 0.1μg of the peptide 2869. A: 10 μg; B: 1 μg; C: 0.1 μg; D: 0.01 μg; E: blank control. (c) IMS of SIO1 treated with purified peptide 2869. A is a photograph of the SIO-1 colonies. B is an IMS picture of *m/z* 2869 $[M+H]^+$, C is *m/z* 1075 $[M+K]^+$, D is *m/z* 1545 $[M+K]^+$, E is a superimposed imaging of A-D, and F is a superimposed imaging of B-D. (d) Two masses, *m/z* 743.5678 $[M+H]^+$ and *m/z* 796.4774 $[M+Fe-2H]^+$, were observed with FT-ICR-MS providing the first indication that this molecule was a siderophore. (e) The structure and 2D NMR correlations of promicroferrioxamine.